

Supporting Information: Electrical Transport and Grain Growth in Solution-Cast, Chloride-Terminated Cadmium Selenide Nanocrystal Thin Films

*Zachariah M. Norman, Nicholas C. Anderson, and Jonathan S. Owen**

Department of Chemistry, Columbia University, 3000 Broadway, New York, NY 10027.
jso2115@columbia.edu

Figure S1. Typical ^1H -NMR spectrum of $\text{CdSe-Cd}(\text{O}_2\text{CR})_2$ 2
Figure S2. Typical ^1H -NMR spectrum of $\text{CdSe-CdCl}_2/\text{PBu}_3$ 2
Figure S3. Typical $^{31}\text{P}\{^1\text{H}\}$ -NMR spectrum of $\text{CdSe-CdCl}_2/\text{PBu}_3$ 3
Figure S4. FTIR spectra of isolated $[(\text{NH}_2\text{Bu})_n(\text{CdCl}_2)]_m$ and reference compounds. 3
Figure S5. Energy dispersive X-ray spectroscopy of $[(\text{NH}_2\text{Bu})_n(\text{CdCl}_2)]_m$ 4
Figure S6. X-ray photoelectron spectroscopy of annealed thin films. 5
Table S1. Elemental analysis of thin film XPS data. 6
Figure S7. Energy dispersive X-ray Spectroscopy of sintered nanocrystal films. 7
Figure S8. Cross sectional transmission electron micrograph of nanocrystalline film after sintering at 200 °C and 300 °C for two hours. 7
Figure S9. Cross sectional SEM of as-cast $\text{CdSe-CdCl}_2/\text{BuNH}_2$ film. 8
Figure S10. Cross sectional SEM of coalesced $\text{CdSe-CdCl}_2/\text{PBu}_3$ film. 9
Figure S11. SEM images of $\text{CdSe-CdCl}_2/\text{NH}_2\text{Bu}$ nanocrystals annealed at 200 °C, 250 °C, and 300 °C. 10
Figure S12. SEM images of $\text{CdSe-CdCl}_2/\text{PBu}_3$ nanocrystal films 11
References. 12

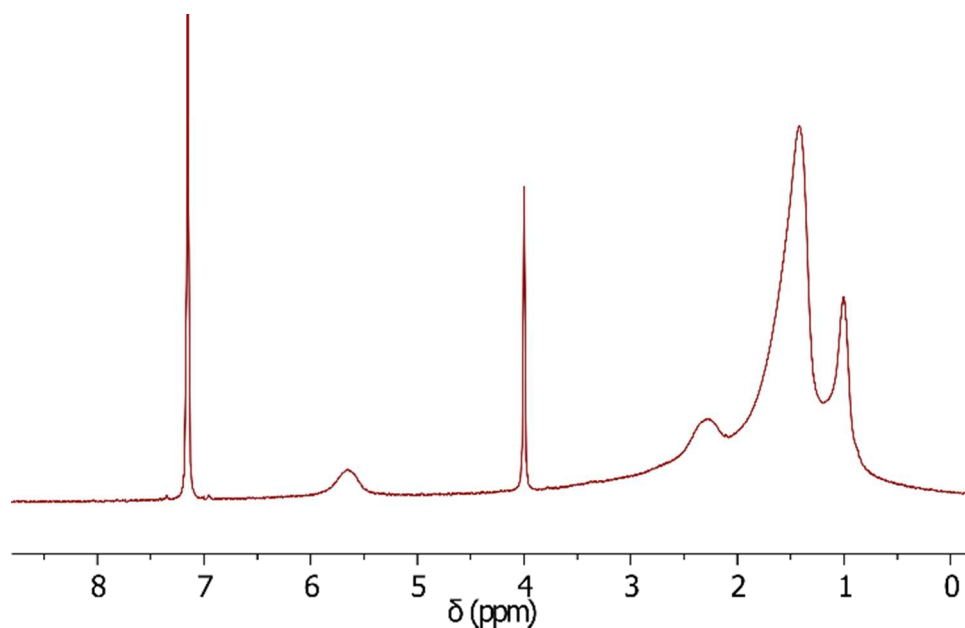


Figure S1. Typical ¹H-NMR spectrum of **CdSe-Cd(O₂CR)₂** shows a mixture of oleyl and tetradecyl moieties bound to the nanocrystal surface. An internal ferrocene concentration standard ($\delta = 4$ ppm) is used to determine the solution ligand concentration.

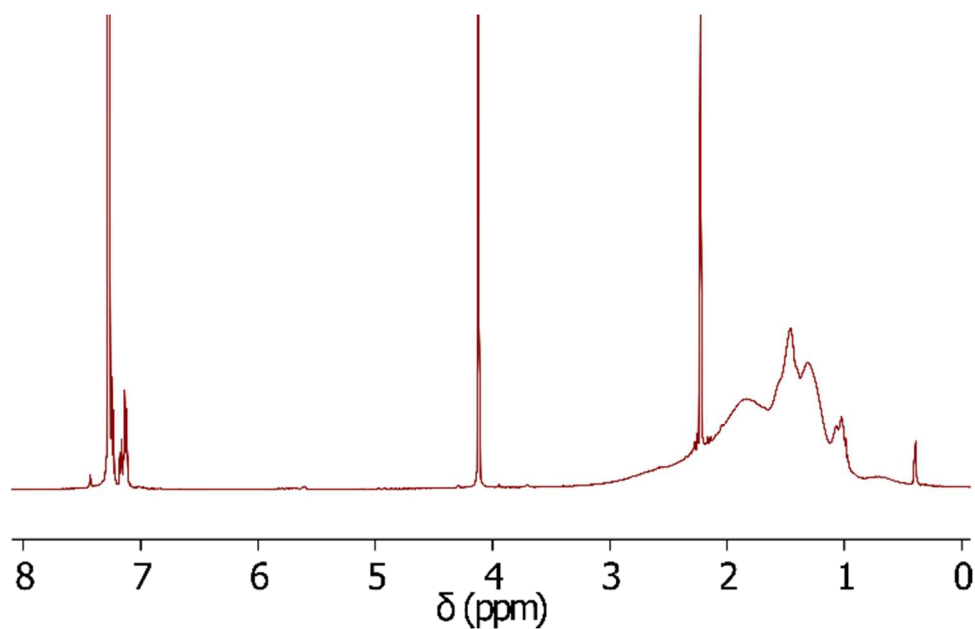


Figure S2. Typical ¹H-NMR spectrum of **CdSe-CdCl₂/PBu₃** shows signals from bound PBu₃ and [Cl]⁻[H-PBu₃]⁺ ligands. An internal ferrocene concentration standard ($\delta = 4$ ppm) is used to determine the solution ligand concentration.

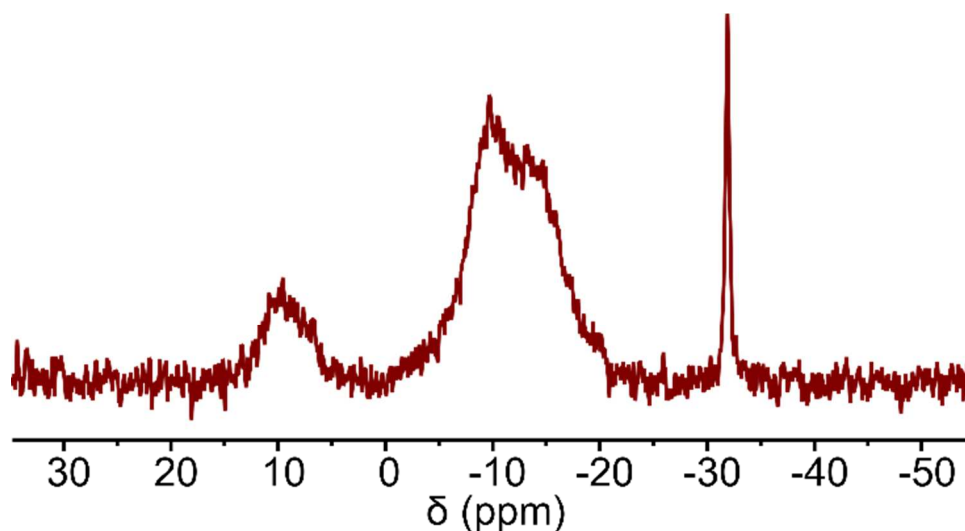


Figure S3. Typical $^{31}\text{P}\{^1\text{H}\}$ -NMR spectrum of **CdSe-CdCl₂/PBu₃** shows four distinct phosphorous resonances due to $[\text{HPBu}_3]^+$ ($\delta = 9.5$ ppm), $\text{PBu}_3:\text{CdCl}_2$ ($\delta = -10.0$ ppm), $\text{CdSe}:\text{PBu}_3$ ($\delta = -14.0$ ppm), and free PBu_3 ($\delta = -32$ ppm).

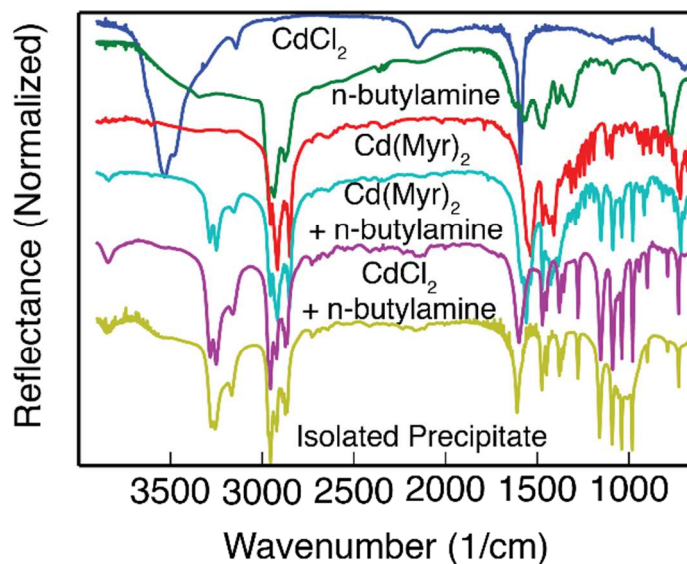


Figure S4. The FTIR spectra of the isolated precipitate, which forms on addition of *n*-butylamine to **CdSe-CdCl₂/PBu₃** nanocrystals, is compared with cadmium chloride, *n*-butylamine, cadmium myristate, cadmium myristate and *n*-butylamine, and cadmium chloride mixed with *n*-butylamine. These spectra suggest strongly that the isolated precipitate is a compound of cadmium chloride and *n*-butylamine ($[(\text{NH}_2\text{Bu})_n(\text{CdCl}_2)]_m$).

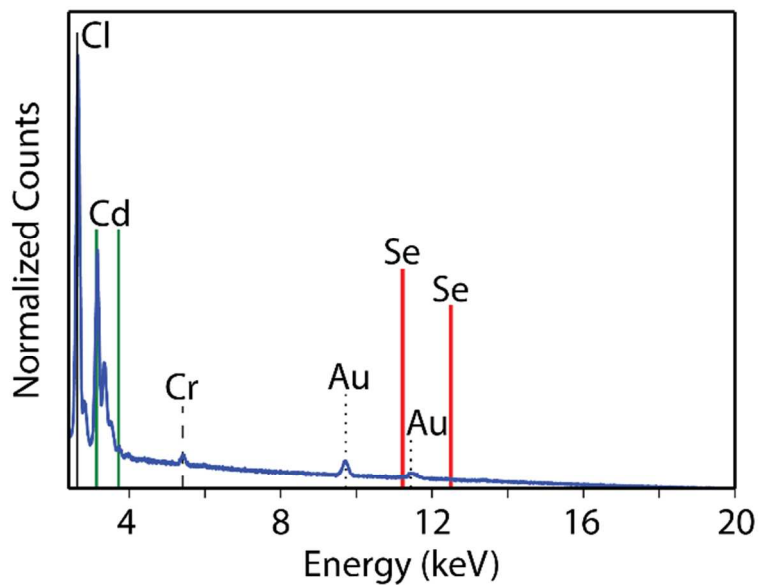


Figure S5. Energy Dispersive x-ray Spectroscopy of $[(\text{NH}_2\text{Bu})_n(\text{CdCl}_2)]_m$ shows signals for only chlorine and cadmium. Signals from chromium and gold are derived from the substrate. No selenium *K* or *L* lines are visible, indicating that the precipitate contains no material from the core of the nanocrystal. The ratio of the signals shows a 1:2:0, Cd:Cl:Se ratio.

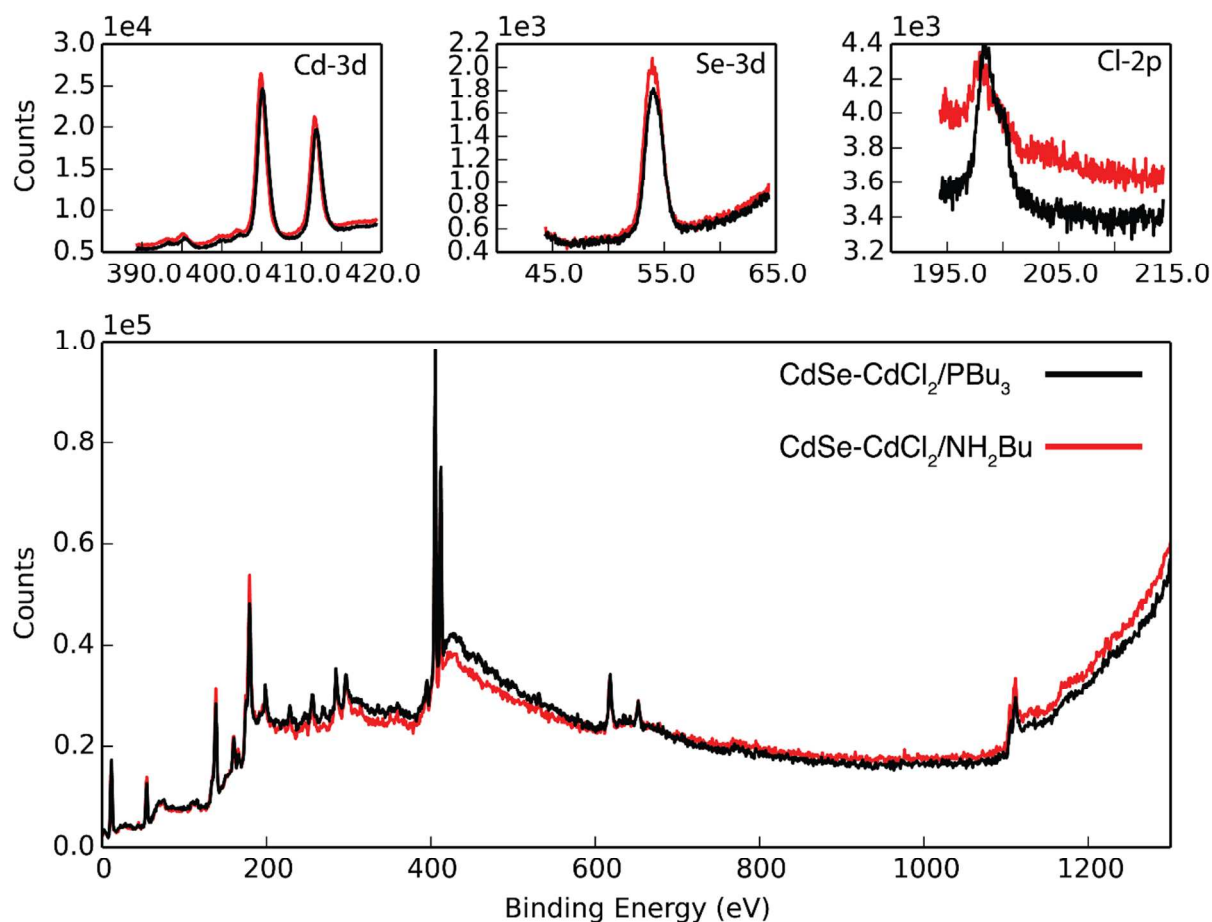


Figure S6. X-ray photoelectron spectroscopy traces of $\text{CdSe-CdCl}_2/\text{BuNH}_2$ and $\text{CdSe-CdCl}_2/\text{PBu}_3$ nanocrystals. The Se-3d, Cl-2p and Cd-3d regions were analyzed by fitting each region to a lorentzian-gaussian lineshape using a Tougaard background.¹ Spin orbit coupling parameters were taken from the NIST X-ray Photoelectron Spectroscopy Database (srdata.nist.gov/xps/).

Table S1. Elemental analysis of thin film XPS data.

Element	Level	Atomic Sensitivity Factor	Binding Energy (eV)	Peak Area	P.A./S.F.	Atom %	Cd/Cl
CdSe-CdCl₂/PBu₃							2.7
Cd	3d 5/2	3.974	405.1	32921	8284	57	
Se	3d	0.853	54.1	2645	3100	21	
Cl	2p	0.891	198.3	2794	3136	22	
CdSe-CdCl₂/NH₂Bu							6.9
Cd	2d 5/2	3.974	401.4	32312	8130	60	
Se	3d	0.853	50.5	3560	4174	31	
Cl	2p	0.891	194	1052	1181	9	
1-(R1/R2)							0.62

Elemental analysis procedure. Elemental composition was calculated from the XPS peak areas. The peak areas were divided by the atomic sensitivity factors for each element to determine the mol % for each element. Comparing the results for **CdSe-CdCl₂/BuNH₂** and **CdSe-CdCl₂/PBu₃** shows a decrease in chlorine content. Because the chloride is on the nanocrystal surface, its signal will be artificially enhanced relative to the interior selenium and cadmium atoms. However, both cadmium chloride and cadmium selenide have similar molar densities (0.022 mol/cm³ and 0.030 mol/cm³ respectively) allowing chlorine signal to be normalized by the cadmium signal in both samples with minimal influence of a change in escape depth. Thus the ratio using the ratios $R = \text{Cd/Cl}$, the quantity $1-R1/R2$ gives the decrease (62%) in the chlorine content between the two samples.

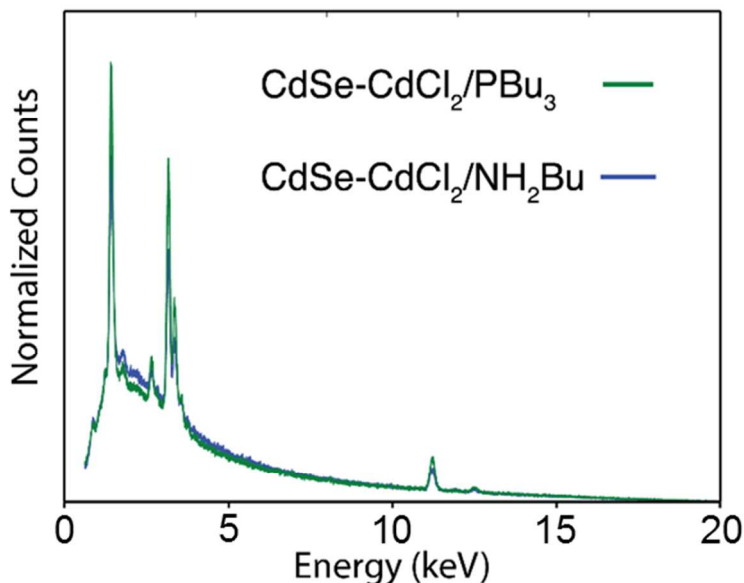
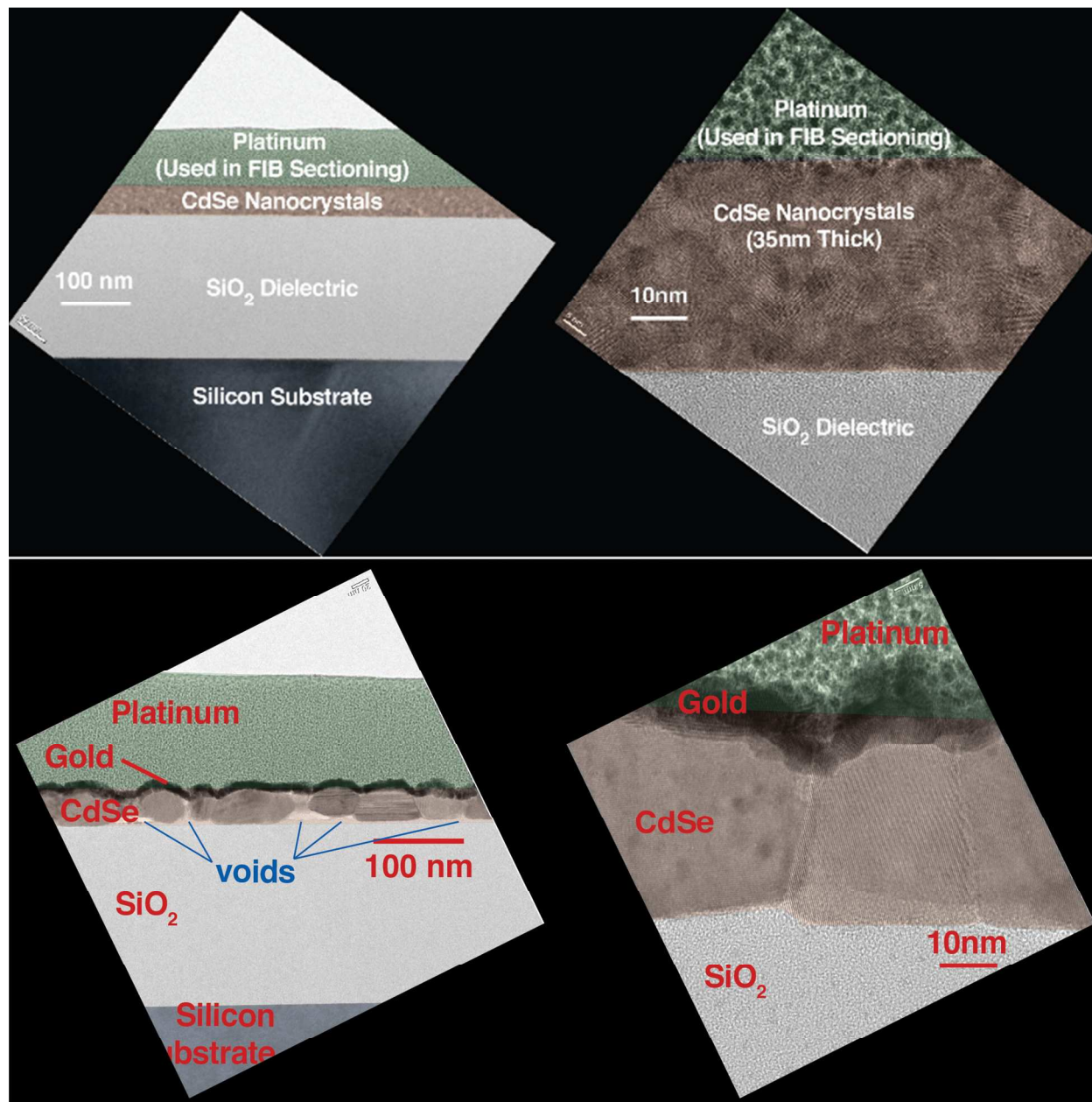


Figure S7. Energy Dispersive x-ray Spectroscopy of sintered films prepared from **CdSe-CdCl₂/PBu₃** and **CdSe-CdCl₂/NH₂Bu** nanocrystals. A reduction in the relative intensity of the chlorine k-alpha line is apparent. Analysis of the selenium *K* lines versus the cadmium *L* and chlorine *K* lines shows atomic composition of 48.2% Cd, 44.0% Se, 7.8% Cl and 48.9% Cd, 47.5% Se, and 3.7% Cl, respectively. The analysis does not change significantly if the selenium *L* lines are analyzed instead. We estimated our uncertainty in this composition by calculating how much chloride there should have been to charge balance the Cd in excess of Se, in which case the Cl⁻ atom % would be 8.4 % and 2.8 % respectively. This means that our EDX data is consistent with chloride concentrations ranging from 7.8 - 8.4 % and 2.8-3.7 % for **CdCl₂/PBu₃** and **CdSe-CdCl₂/NH₂Bu** respectively, which we report as 8 % and 3 %.



Figures S8. Cross sectional transmission electron micrographs of sections of films prepared from $\text{CdSe-CdCl}_2/\text{PBU}_3$ annealed for 2 hours at 200 °C (top) and 300 °C (bottom). At 200 °C the nanocrystals are randomly, but densely packed. Annealing at 300 °C produces grains that extend the entire thickness of the film. Void spaces between the grains and between the grains and the substrate are also apparent.

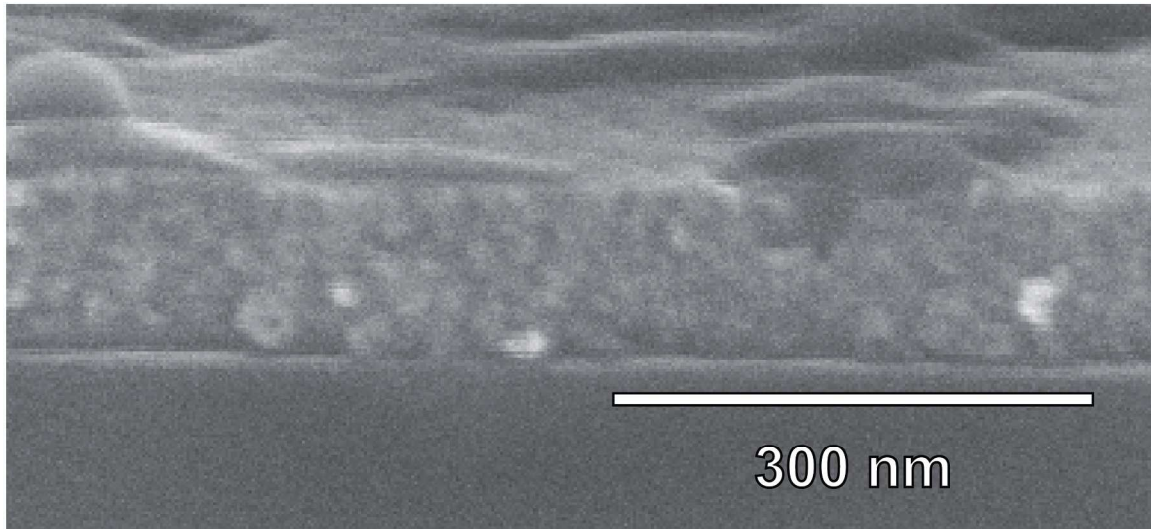


Figure S9. Cross sectional SEM of as-cast $\text{CdSe-CdCl}_2/\text{BuNH}_2$ film show a randomly, close-packed assembly of particles 100 nm thick.

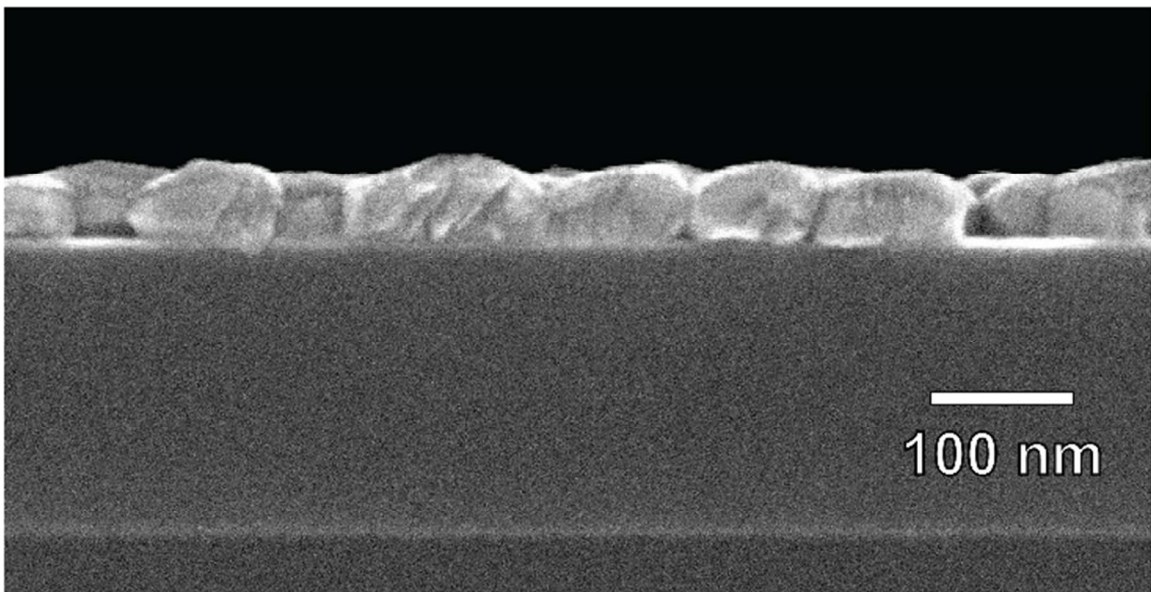


Figure S10. Cross sectional SEM of $\text{CdSe-CdCl}_2/\text{PBu}_3$ film heated to 300 °C showing large grains extending the entire thickness of the film. Void spaces are observable between grains and near the dielectric interface.

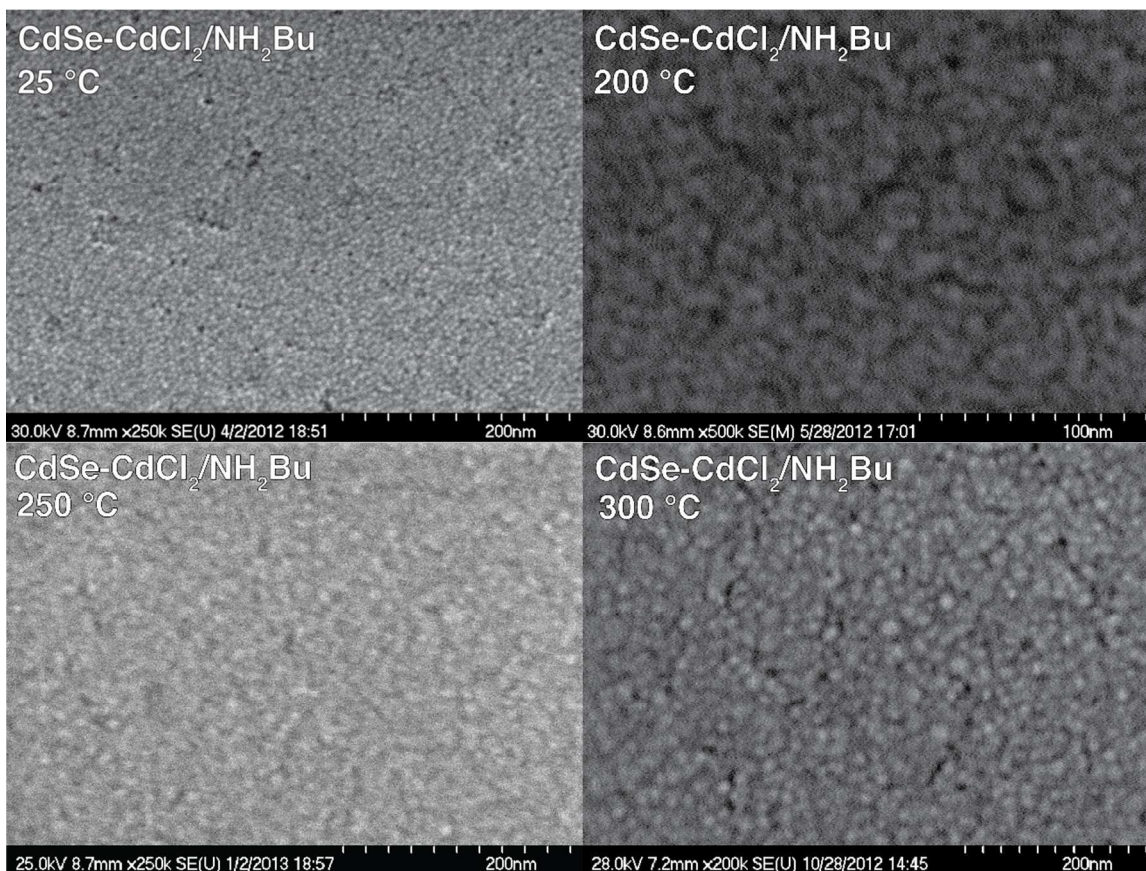


Figure S11. Normal incident SEM images of CdSe-CdCl₂/NH₂Bu nanocrystal films annealed at room temperature, 200 °C, 250 °C, and 300 °C for two hours each. Annealing does not lead to the formation of cracks. Nanometer scale grains are readily apparent at all annealing temperatures and remain less than 10 nm below 300 °C.

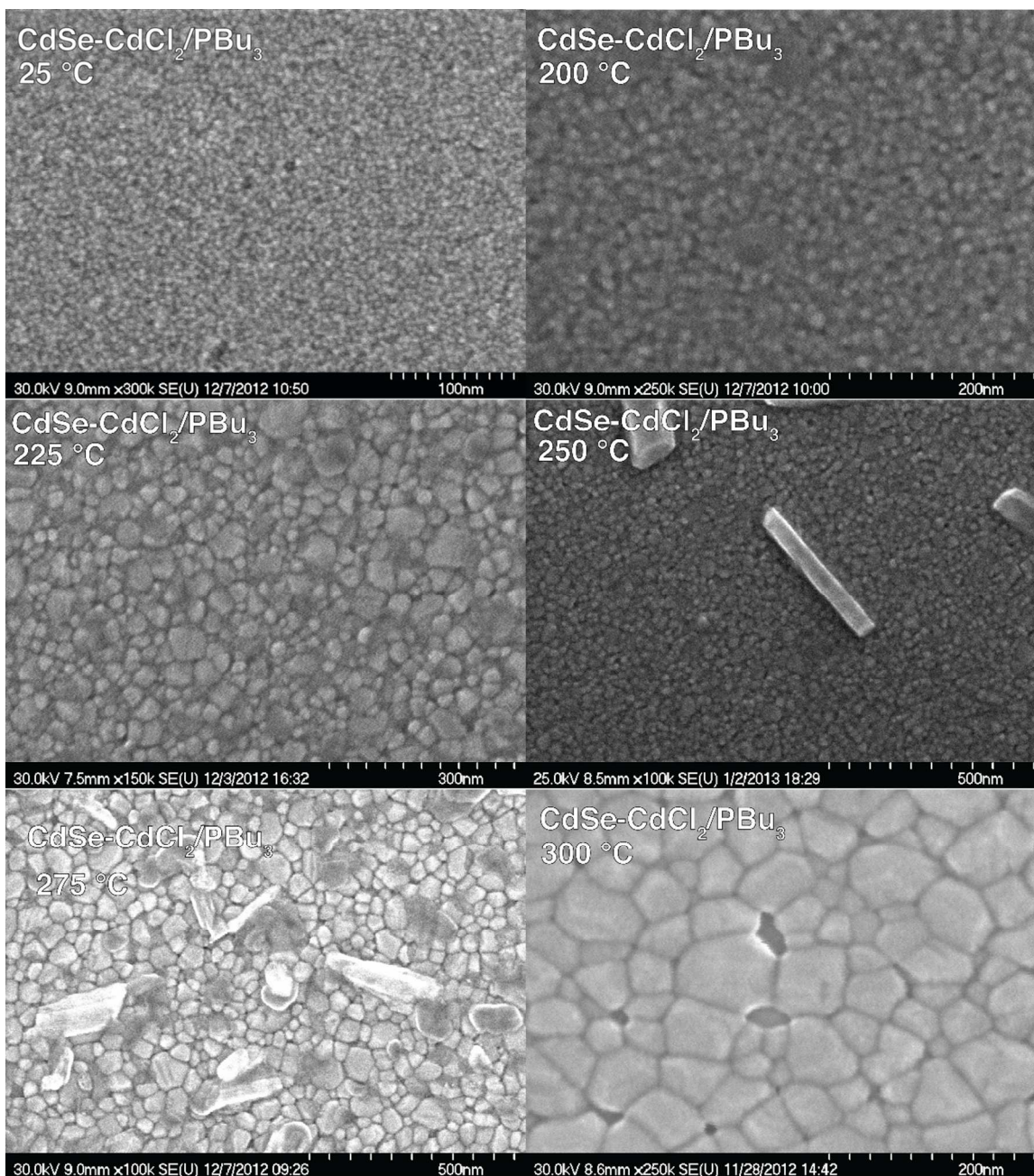


Figure S12. Normal incident SEM images of CdSe-CdCl₂/PBu₃ nanocrystal films annealed at room temperature, 200 °C, 225 °C, 250 °C, 275 °C, and 300 °C. Needle-like crystallites at higher temperatures are hypothesized to be cadmium chloride, which is observed in the wide-angle x-ray diffraction pattern at these temperatures. Crystallites proved too small for spatially resolved elemental mapping by EDX.

References.

- (1) Seah, M. P. Background Subtraction: I. General Behaviour of Tougaard-Style Backgrounds in AES and XPS. *Surf. Sci.* **1999**, *420*, 285–294.